# Biodistribution and Absorbed Radiation Dose Estimates of $^{99m}$Tc-Labeled Dimercaptopropionyl Human Serum Albumin

Andries van Aswegen, Johan Marais, Gerdus Kemp, Mariana G. Nel, Johan A. van Staden, Anton C. Otto, Mattheus G. Lötter and Alfons M. Verbruggen

*Departments of Medical Physics and Nuclear Medicine, University of the Orange Free State, Bloemfontein, South Africa; and Department of Radiopharmacy, University of Leuven, Leuven, Belgium*

The use of $^{99m}$Tc-labeled red blood cells (RBC) for the evaluation of left ventricular function using equilibrium-gated blood-pool imaging suffers from several problems and potential risks. In this study, we estimated the absorbed radiation dose of $^{99m}$Tc-labeled dimercaptopropionyl human serum albumin (DMP-HSA) as a potential alternative to $^{99m}$Tc-RBC. **Methods:** After the administration of $^{99m}$Tc-DMP-HSA, whole-body imaging was performed up to 48 h after injection in five volunteers. The heart contents, liver and remainder of the body were used as source organs. Multicompartment modeling of the biodistribution was performed and absorbed radiation dose estimates for $^{99m}$Tc-DMP-HSA were obtained using the Medical Internal Radiation Dose (MIRD) calculation. **Results:** Residence times of 0.62 and 0.43 h were obtained for the heart contents and liver, respectively. Radiation dose estimates yielded an effective dose of 0.0055 mSv/MBq. **Conclusion:** $^{99m}$Tc-DMP-HSA yielded absorbed radiation doses comparable with those of $^{99m}$Tc-RBC. Therefore, the radiation properties of $^{99m}$Tc-DMP-HSA are such that it can be used for clinical diagnostic studies.

**Key Words:** $^{99m}$Tc blood-pool labeling; dosimetry; Medical Internal Radiation Dose; $^{99m}$Tc-labeled dimercaptopropionyl human serum albumin

**J Nucl Med 1999; 40:1532–1535**

Noninvasive radionuclide multigated blood-pool imaging at equilibrium is still widely used in clinical practice for several reasons. These include objective determination of global left ventricular (LV) systolic function (LV ejection fraction and rate), LV size and wall motion, LV diastolic function, right ventricular size and function as well as determination of the presence of possible pericardial disease (*1–3*). Studies often must be performed in succession, for instance, to evaluate a patient's response to drug therapy (usually performed at rest) (*4,5*) or to evaluate possible ischemic heart disease (performed during rest and exercise) (*6,7*). To obtain reliable results, it is imperative that the radionuclide blood-pool label remain in the blood pool for the total duration of the examination.

$^{99m}$Tc-labeled human serum albumin (HSA) was originally used as the blood-pool labeling agent (*8*) because the HSA diffuses into the plasma component of the blood. Unfortunately, the binding of the radionuclide to this protein is relatively weak, resulting in a rapid extravascular diffusion. Furthermore, high liver uptake occurs, impeding the accurate determination of the LV inferior border; this contributes to making this blood-pool marker unsatisfactory for multigated blood-pool imaging.

The development of efficient methods for labeling of red blood cells (RBCs) with $^{99m}$Tc resulted in the multigated blood-pool study being established as one of the primary screening investigations for evaluating patients with functional cardiac disease. Labeling of RBCs with $^{99m}$Tc can be performed either by in vivo or in vitro methods (*9,10*). The labeling efficiency of the in vivo method often is not high and can be influenced negatively by certain drugs (*11*) or even by the injection technique (*12*), resulting in images with low target-to-background count ratios. On the other hand, labeling efficiencies of >90% are usually obtained with the in vitro method. Although the in vitro method yields the best results, certain hazards are associated with it. These hazards include, among others, the following. First, it requires that the blood be handled by nuclear medicine technologists, increasing the risk of contamination with the hepatitis B or AIDS viruses. Second, the possibility exists that patients' blood samples could be interchanged when more than one patient's blood is labeled simultaneously, especially in departments with high workloads.

It would be a major advantage in the performance of multigated blood-pool imaging if the tracer agent could be reconstituted from a labeling kit and could be available on demand with the least loss of time to start the study. Verbeke et al. (*13,14*) reported the development and evaluation of a derivative of $^{99m}$Tc-HSA that is more stable in blood and stays in the circulation nearly as well as $^{99m}$Tc-labeled RBCs, namely $^{99m}$Tc-dimercaptopropionyl (DMP) HSA. Hambÿe et

Received Sept. 24, 1998; revision accepted Mar. 8, 1999.

For correspondence or reprints contact: Andries van Aswegen, PhD, Department of Medical Physics, University of the Orange Free State, P.O. Box 339, 9300 Bloemfontein, South Africa.

al. (*15*) reported the clinical use of $^{99m}$Tc-DMP-HSA, which meets the aforementioned requirements of an ideal labeling agent. In this study, the biodistribution and patient radiation dose estimates of $^{99m}$Tc-DMP-HSA were determined.

## METHODS

### Patients

Five healthy men were enrolled in the study on a voluntary basis. Their ages ranged from 26 to 31 y (mean 28.2 ± 1.7 y), and they weighed between 65 and 100 kg (mean 89.6 ±11.6 kg). No volunteer was using any medication. The Ethics Committee and Radiation Control Committee of the University of the Orange Free State approved the study protocol and permission was obtained from the Medicines Control Council of South Africa for use of the $^{99m}$Tc-labeled DMP-HSA. Informed written consent was obtained from each volunteer.

### Radiopharmaceutical

Labeling kits for the preparation of $^{99m}$Tc-DMP-HSA were obtained from the Radiopharmacy Department of the University of Leuven, Belgium (*16*). Labeling of DMP-HSA with $^{99m}$Tc was a three-step procedure. First, the DMP-HSA kit was reconstituted by the addition of 1–5 mL (925–3700 MBq) freshly eluted $^{99m}$Tc-pertechnetate (Peltek-F; Atomic Energy Corp., Pelindaba, South Africa). Second, 10 mL saline were added to a vial containing Sn-diethylenetriamine pentaacetic acid (DTPA) and the Sn-DTPA was completely dissolved. Last, 0.25 mL of the Sn-DTPA solution was added to the vial containing the $^{99m}$Tc-DMP-HSA. Labeling efficiency was determined according to the method described by Verbeke et al. (*16*) using thin-layer chromatography strips with acetone and acid-citrate-dextrose solution as mobile phases to determine the percentage of free $^{99m}$Tc-pertechnetate and labeled $^{99m}$Tc-DMP-HSA. A total activity (bound plus unbound $^{99m}$Tc) of approximately 740 MBq $^{99m}$Tc-DMP-HSA was administered intravenously to each volunteer.

### Data Acquisition

Imaging was performed with a dual-detector scintillation camera system (Multispect 2; Siemens, Hoffman Estates, IL) with the patient in the supine position. The camera was fitted with low-energy high-resolution collimators. A 15% energy window was positioned over the 140-keV photopeak for $^{99m}$Tc.

After the intravenous administration of the radiopharmaceutical, whole-body anterior and posterior images were acquired simultaneously in 1024 × 256 matrices using a scan speed of 8 cm/min. This yielded a total count of almost 1 million in each image with an acquisition time of about 20 min per scan. Similar images were acquired with the same scan speed at 3, 6, 24, 30 and 48 h.

### Data Processing

As a result of the whole-body distribution of $^{99m}$Tc-DMP-HSA, the heart, liver and remainder of the body were used as source organs. (Although some bladder and kidney uptake was seen in the early images in some cases, this uptake was relative low, and we decided not to use these as separate source organs but to include the uptake in the remainder counts.) The first whole-body scan was used as the 100% activity uptake value and the anterior and posterior images were analyzed separately. Regions of interest were drawn around the heart, the liver and the whole body. The counts in the heart and the liver were subtracted from the whole-body counts to obtain the counts for the remainder of the body. The geometric mean counts (i.e., the square root of the product of the anterior and posterior counts) were calculated for each source organ, expressed as a percentage of the whole-body activity and normalized to the 100% value obtained from the first whole-body image. The arithmetic mean percentage uptakes in the various source organs of the five volunteers were used for further calculations.

The biokinetics of $^{99m}$Tc-DMP-HSA were determined using a multicompartment model consisting of three compartments, one each for the blood, the liver and the remainder of the body. The simulation analysis and modeling were performed with the SAAM30 software (Washington State University, Seattle, WA). The areas under the modeled time-activity curves for the different source organs were calculated to obtain the biological washout. Source organ elimination by physical decay alone was assumed to occur from the last measured time point. The biological removal and physical decay data were used to yield the mean residence times of the radionuclide in the different source organs. Subsequently, these data were used as input data to calculate radiation dose estimates for $^{99m}$Tc-DMP-HSA according to the Medical Internal Radiation Dose (MIRD) schema (*17*) using the MIRDOSE 3.1 software (*18*) that incorporated the dynamic bladder model. This model assumes that the bladder is voided every 3 h during the first 12 h after the administration of the radiopharmaceutical.

## RESULTS

### Labeling Efficiency

The mean percentage of $^{99m}$Tc bound to DMP-HSA after reconstitution was 95.1% ± 1.8%, ranging from 92.5% to 98.4%.

### Biodistribution

The whole-body distribution of $^{99m}$Tc-DMP-HSA and that of $^{99m}$Tc-RBC from a volunteer study is shown in Figure 1. Figure 2 indicates the mean time-activity curves of $^{99m}$Tc-DMP-HSA obtained for the heart and liver. Uptake values in these respective organs were 9.6% and 10.0% in the first image and 5.2% and 7.6% after 48 h.

### Radiation Dose Estimation

The residence times obtained for $^{99m}$Tc-DMP-HSA in the heart contents, liver and remainder of the body were 0.62, 0.43 and 8.47 h, respectively. The absorbed radiation dose estimates for $^{99m}$Tc-DMP-HSA are given in Table 1. $^{99m}$Tc-DMP-HSA yielded an effective dose of 0.0055 mSv/MBq. Therefore, for a typical 740 MBq administration of $^{99m}$Tc-DMP-HSA, the absorbed radiation dose to the heart wall, spleen, lungs, liver, kidneys and red marrow will be 12.43, 3.86, 4.13, 5.72, 3.89 and 3.54 mGy, respectively. A total effective dose of 4.07 mSv will be delivered.

## DISCUSSION

In this study, the radiation dose estimates associated with blood-pool labeling with $^{99m}$Tc-DMP-HSA were calculated. The use of $^{99m}$Tc-DMP-HSA has advantages over $^{99m}$Tc-RBC: The radiopharmaceutical can be reconstituted with a labeling kit for instant use, and there is no direct handling of the patient's blood, eliminating the associated hazards.

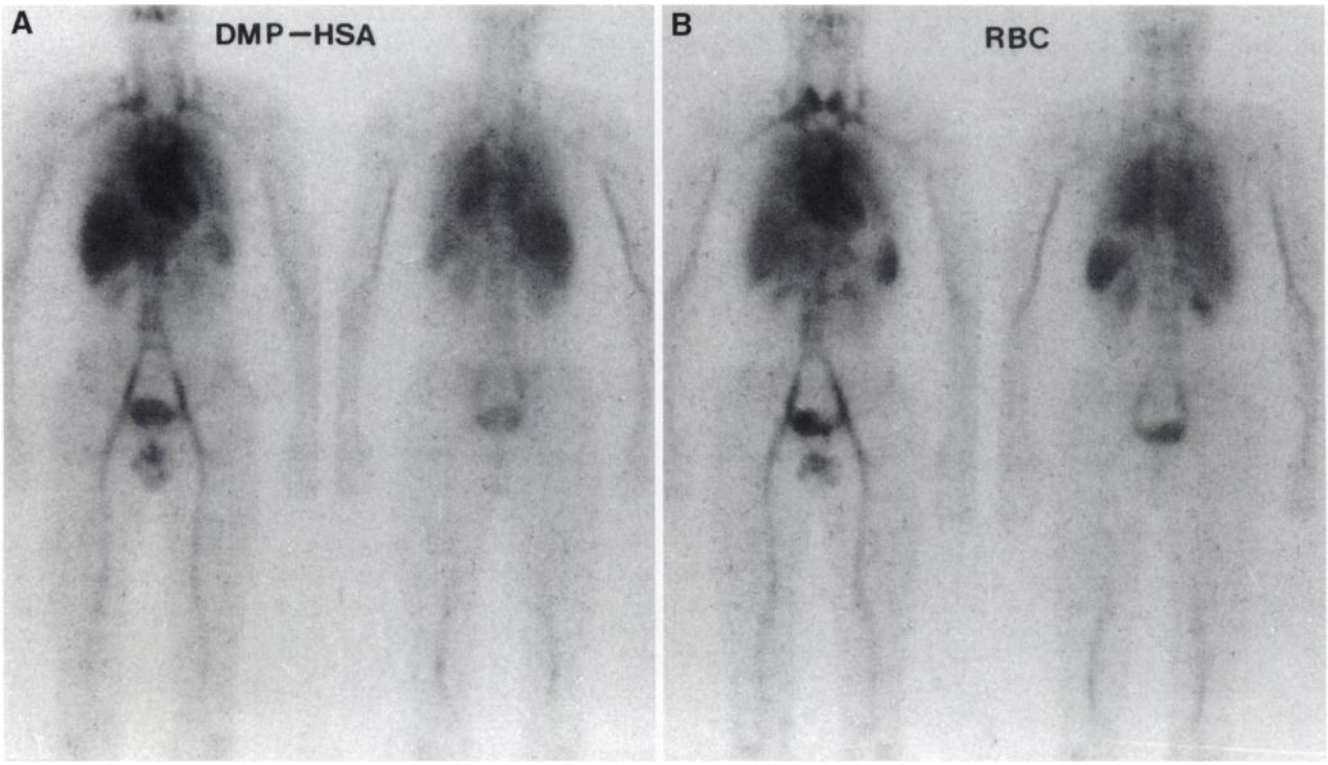


**FIGURE 1.** Typical whole-body anterior (left) and posterior (right) scans obtained in same individual with (A) $^{99m}$Tc-labeled dimercaptopropionyl human serum albumin ($^{99m}$Tc-DMP-HSA) (1 h postinjection) and (B) $^{99m}$Tc-labeled red blood cells ($^{99m}$Tc-RBC) (7 d before $^{99m}$Tc-DMP-HSA study).

Furthermore, a high labeling efficiency of $^{99m}$Tc to DMP-HSA (range 92.5%–98.4%) was obtained that corresponds well with reported values >95% for in vitro-labeled $^{99m}$Tc-RBC (*19*).

Residence times obtained for $^{99m}$Tc-DMP-HSA in this study compared well with those reported by Russell et al. (*20*) for $^{99m}$Tc-RBC and $^{99m}$Tc-HSA. The residence times for the heart contents for $^{99m}$Tc-RBC were 0.57 h (in vitro labeling) and 0.864 h (in vivo labeling), whereas the residence time for $^{99m}$Tc-HSA was reported to be 0.813 h compared with 0.622 h obtained in this study for $^{99m}$Tc-DMP-HSA. The longer residence time of $^{99m}$Tc-HSA could be due

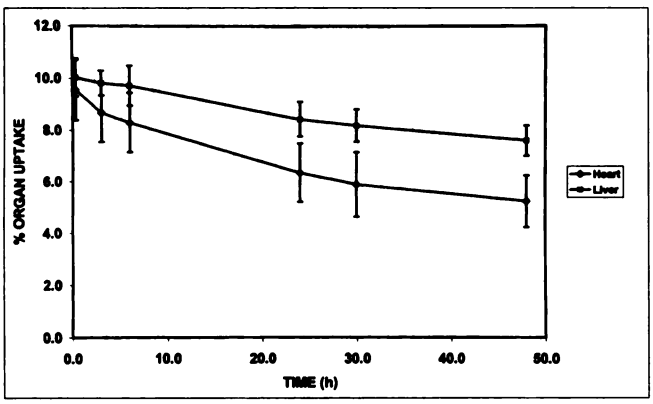


**FIGURE 2.** Mean (n = 5) uptake time-activity curves of $^{99m}$Tc-DMP-HSA obtained for heart (bottom curve) and liver (top curve) according to multicompartment analysis.

**TABLE 1**
Radiation Absorbed Dose Estimates for $^{99m}$Tc-DMP-HSA

| Target organ | Absorbed dose (mGy/MBq) |
|---|---|
| Adrenals | 0.0062 |
| Brain | 0.0039 |
| Breasts | 0.0038 |
| Gallbladder wall | 0.0065 |
| LLI wall | 0.0055 |
| Small intestine | 0.0057 |
| Stomach | 0.0055 |
| ULI wall | 0.0056 |
| Heart wall | 0.0168 |
| Kidneys | 0.0053 |
| Liver | 0.0077 |
| Lungs | 0.0056 |
| Muscle | 0.0044 |
| Ovaries | 0.0058 |
| Pancreas | 0.0065 |
| Red marrow | 0.0048 |
| Bone surfaces | 0.0085 |
| Skin | 0.0030 |
| Spleen | 0.0052 |
| Testes | 0.0041 |
| Thymus | 0.0064 |
| Thyroid | 0.0048 |
| Urinary bladder wall | 0.0053 |
| Uterus | 0.0058 |
| Total body | 0.0048 |

DMP-HSA = dimercaptopropionyl human serum albumin; LLI = lower large intestine; ULI = upper large intestine.

to its extravascular diffusion. In vitro-labeled $^{99m}$Tc-RBC and $^{99m}$Tc-DMP-HSA both have high labeling efficiencies, and because they stay intact in the blood, the residence times are similar. Furthermore, residence times for in vitro- and in vivo-labeled $^{99m}$Tc-RBC for the liver were 0.322 and 0.334 h, respectively, and residence time for $^{99m}$Tc-HSA was 0.457 h. In this study, the residence time for $^{99m}$Tc-DMP-HSA was 0.428 h.

The estimated absorbed organ doses obtained for $^{99m}$Tc-DMP-HSA compare favorably with those reported by Atkins et al. (*21*) for $^{99m}$Tc-RBC. The absorbed doses for the respective radiopharmaceuticals to the various organs were as follows: heart wall, 0.0168 and 0.015 mGy/MBq; spleen, 0.0052 and 0.011 mGy/MBq; lungs, 0.0056 and 0.011 mGy/MBq; liver, 0.0077 and 0.0070 mGy/MBq; kidneys, 0.0053 and 0.0068 mGy/MBq; and red marrow, 0.0048 and 0.0051 mGy/MBq. The $^{99m}$Tc-RBC values are for in vitro-labeled RBCs and a 2.4-h voiding schedule. The higher $^{99m}$Tc-RBC dose to the spleen is probably due to the accumulation of RBCs in the organ. This could also be the reason for the higher dose to the lungs, because the spleen will be a source organ (situated relatively close to the lungs) with $^{99m}$Tc-RBC and will not be a source organ with $^{99m}$Tc-DMP-HSA.

The effective dose of 0.0055 mSv/MBq that is obtained with $^{99m}$Tc-DMP-HSA is lower than the effective dose of 0.0098 mSv/MBq that is obtained for $^{99m}$Tc-labeled erythrocytes and 0.0088 mSv/MBq that is reported by Johansson et al. (*22*) for $^{99m}$Tc-HSA. The higher effective dose of $^{99m}$Tc-labeled erythrocytes compared with $^{99m}$Tc-DMP-HSA could be due to the accumulation and extended retention of the RBCs in the spleen as a source organ. Likewise, the high uptake of HSA in the liver as source organ and increased uptake in the remainder of the body due to the extravascular diffusion could contribute to the higher effective dose reported for $^{99m}$Tc-HSA compared with $^{99m}$Tc-DMP-HSA found in this study. Furthermore, internal radiation dose estimation is subject to a certain magnitude of error. Errors on the calculation of the percentage organ uptake and effective half-life of the radiopharmaceutical, for instance, will contribute to a combined error on the absorbed radiation dose (*23*). This is illustrated in reports on the dose estimates of $^{123}$I-fluoropropyl-carbomethoxy-iodophenyl-tropane (FPCIT) in healthy participants in which effective dose values of 0.024 mSv/MBq (*24*) and 0.041 mSv/MBq (*25*) were stated.

## CONCLUSION

The new modified HSA blood-pool-labeling agent $^{99m}$Tc-DMP-HSA yielded absorbed radiation doses comparable with those of $^{99m}$Tc-RBC. Therefore, it may be concluded that, due to its radiation properties, $^{99m}$Tc-DMP-HSA can be considered as a practical blood-pool-labeling agent for the evaluation of LV function.

## REFERENCES


1. Bartlett ML, Srinivasan G, Barker WC, Kitsiou AN, Dilsizian V, Bacharach SL. Left ventricular ejection fraction: comparison of results from planar and SPECT gated blood-pool studies. *J Nucl Med.* 1996;37:1795–1799.
2. Petersen CL, Gadsbøll N, Stadeager C, et al. Changes in left and right ventricular performance and volumes in seven-year survivors of acute myocardial infarction. *Am J Cardiol.* 1995;75:659–664.
3. Dilsizian V, Rocco TP, Bonow RO, Fischman AJ, Boucher CA, Strauss HW. Cardiac blood-pool imaging. II. Applications in noncoronary heart disease. *J Nucl Med.* 1990;31:10–22.
4. Herbst CP, Otto AC, van Aswegen A, Sweetlove A, Strugo V. A comparison of the acute hemodynamic effects of nifedipine and nisoldipine in patients with ischemic reduced left ventricular function. *Eur J Nucl Med.* 1987;13:72–75.
5. Otto AC, van Aswegen A, Herbst CP, Sweetlove MA, Viviers AC, Flint GR. The effects of nisoldipine on left ventricular filling rate in patients with ischemic heart disease measured with radionuclide gated blood pool scintigraphy. *Eur J Nucl Med.* 1988;14:542–545.
6. Borer JS, Bacharach SL, Green MV, Kent KM, Epstein SE, Johnston GS. Real-time radionuclide cineangiography in the noninvasive evaluation of global and regional left ventricular function at rest and during exercise in patients with coronary-artery disease. *N Engl J Med.* 1977;296:839–844.
7. Rocco TP, Dilsizian V, Fischman AJ, Strauss HW. Evaluation of ventricular function in patients with coronary artery disease. *J Nucl Med.* 1989;30:1149–1165.
8. van Aswegen A, Kleynhans PHT, Lötter MG, Minnaar PC, Iturralde M. Global and regional assessment of cardiac performance by ECG-gated radionuclide blood pool imaging. *S Afr Med J.* 1979;56:50–53.
9. Chervu LR. Radiopharmaceuticals in cardiovascular nuclear medicine. *Semin Nucl Med.* 1979;9:241–256.
10. Pavel DG, Zimmer AM, Patterson VN. In vivo labeling of red blood cells with $^{99m}$Tc: a new approach to blood pool visualization. *J Nucl Med.* 1977;18:305–308.
11. Lee HB, Wexler JP, Scharf SC, Blaufox MD. Pharmacologic alterations in $^{99m}$Tc binding by red blood cells: concise communication. *J Nucl Med.* 1983;24:397–401.
12. Verbeke K, Verbruggen A. Failure of in vivo labelling of erythrocytes with technetium-99m: it is not Teflon that is the problem but rather the injection technique. *Eur J Nucl Med.* 1997;24:448.
13. Verbeke KA, Vanbilloen HP, De Roo MJ, Verbruggen AM. Technetium-99m mercaptoalbumin as a potential substitute for technetium-99m labelled red blood cells. *Eur J Nucl Med.* 1993;20:473–482.
14. Verbeke KA, Vanhecke WJ, Mortelmans LA, Verbruggen AM. First evaluation of technetium-99m dimercaptopropionyl albumin as a possible tracer agent for ventriculography in a volunteer. *Eur J Nucl Med.* 1994;21:906–912.
15. Hambÿe AE, Verbeke KA, Vandermeiren RP, Joosens EJ, Verbruggen AM, De Roo MJ. Comparison of modified technetium-99m albumin and technetium-99m RBC for equilibrium ventriculography. *J Nucl Med.* 1997;38:1521–1528.
16. Verbeke KA, Schiepers CW, Wyndacle DN, et al. Development and evaluation of a kit formulation for the preparation of $^{99m}$Tc DMP-HSA, a new tracer agent for radionuclide ventriculography. *Nucl Med Biol.* 1997;24:571–578.
17. Loevinger R, Budinger TF, Watson EE. *MIRD Primer for Absorbed Dose Calculation.* Rev ed. New York, NY: Society of Nuclear Medicine; 1991.
18. Stabin MG. MIRDOSE: personal computer software for internal dose assessment in nuclear medicine. *J Nucl Med.* 1996;38:538–546.
19. Srivastava SC, Straub RF. Blood cell labeling with $^{99m}$Tc: progress and perspectives. *Semin Nucl Med.* 1990;20:41–51.
20. Russell JR, Stabin MG, Sparks RB, Watson E. Radiation absorbed dose to the embryo/fetus from radiopharmaceuticals. *Health Phys.* 1997;73:756–769.
21. Atkins HL, Thomas SR, Buddemeyer U, Chervu LR. MIRD dose estimate report no. 14: radiation absorbed dose from technetium-99m-labeled red blood cells. *J Nucl Med.* 1990;31:378–380.
22. Johansson L, Mattsson S, Nosslin B, Leide-Svegborn S. Effective dose from radiopharmaceuticals. *Eur J Nucl Med.* 1992;19:933–938.
23. Flower MA, McCready VR. Radionuclide therapy dose calculations: what accuracy can be achieved? *Eur J Nucl Med.* 1997;24:1462–1464.
24. Booij J, Busemann Sokole E, Stabin MG, Janssen AGM, de Bruin K, van Royen EA. Human biodistribution and dosimetry of [$^{123}$I]FP-CIT: a potent radioligand for imaging of dopamine transporters. *Eur J Nucl Med.* 1998;25:24–30.
25. Abi-Dargham A, Innis RB, Wisniewski G, Baldwin RM, Neumeyer JL, Seibyl JP. Human biodistribution and dosimetry of iodine-123-fluoroalkyl analogs of β-CIT. *Eur J Nucl Med.* 1997;24:1422–1425.